ORIGINAL RESEARCH ARTICLE

Experimental study of contrast-enhanced ultrasound in the evaluation of random-pattern flap blood supply in the early postoperative stage in rats

Jian-Xun Ma[a#], You-Chen Xia[a#], Zhi-Yong Bai[b], Hua-Bin Zhang[b] and Xia Xie[b]

[a]Department of Plastic Surgery, Peking University Third Hospital, Beijing, China; [b]Department of Ultrasound, Beijing Tsinghua Changgung Hospital, Beijing, China

ABSTRACT

Purpose: This study aims to investigate whether contrast-enhanced ultrasound (CEUS) could be used to reveal the status of blood supply of the superficial flap of rat model in the early postoperative stage.
Methods: One viable and one ischemic random-pattern flap were prepared on the left and right back of the same rat respectively with a number of 40. CEUS examinations were applied within 12 h and 7 days postoperatively, and the quantitative measurements of microvascular blood volume (BV) of the base and the end of both flaps were expressed using acoustic intensity as a ratio to that of the healthy skin.
Results: Within 12 h post operation, there was a smaller BV value of the ischemic ends than that of both the ischemic bases and viable ends ($p < 0.001$), while no difference was indicated between ischemic bases and viable bases or between viable bases and viable ends. The same result was provided 7 days post operation.
Conclusion: Microcirculation of superficial tissues such as random-pattern flaps in this rat model can be assessed quantitatively by CEUS. It could sensitively and accurately reveal the objective status of tissue perfusion in the early postoperative stage.

Introduction

Flap transplantation is one of the most commonly used methods of tissue repair in plastic surgery, but there are still some problems that might be encountered in clinical practice, especially disorders of blood supply. The early detection of the failure of flap transplantation caused by abnormal blood circulation and immediate intervention to restore tissue perfusion could usually prevent the loss of flaps [1]. Therefore, it is particularly important to effectively assess the tissue perfusion of skin flaps after transplantation, determine problems in the early stage and take appropriate measures in time.

Generally, the blood supply of the transplanted skin flaps is evaluated mainly by the assessment of the flap color, temperature, capillary recirculate time, and bleeding during pinprick [2]. Although these methods are relatively convenient, they require the observers to have rich clinical experience, and they mainly depend on subjective judgment but not objective indicators. Currently, many other methods to evaluate the blood supply of flaps have emerged. However, most of them have some disadvantages, such as a lack of objective evaluation indexes, poor practicability, and invasiveness [3–8]. Therefore, more effective and objective methods for monitoring the blood supply of transplanted skin flaps have been sought. These methods should be highly sensitive, reliable, and not harmful to patients.

In the last decade, contrast-enhanced ultrasound (CEUS) has emerged as a valuable diagnostic tool to evaluate dynamic changes in capillary blood flow [9, 10]. In this study, an animal model was established in which both well-designed ischemic and viable random-pattern skin flaps coexisted, and CEUS was performed in the early postoperative stage. Through the analysis of the data of relevant perfusion indexes, we explored whether the perfusion indexes of CEUS correlate with the actual circulation status of these two well-designed ischemic and viable random-pattern skin flaps after transplantation to clarify the role of CEUS in the evaluation and monitoring of the flap blood supply in the early period postoperatively.

Material and methods

Animals

Forty healthy male Sprague-Dawley rats weighing 350–400 g were housed in the Experimental Animal Center of the Peking University Health Science Center. All animals were given rat chow ad libitum.

This study was conducted in accordance with the Guide for the Care and Use of Laboratory Animals and was approved by the Animal Ethics Committee of the Peking University Health Science Center (ethics approval number: LA2013-83).

Establishment of animal model

Each rat was anesthetized by intraperitoneal administration of 0.3% sodium pentobarbital at a dose of 0.1 mL per 100 g. The surgical site was prepared by shaving the back and disinfecting the skin with conventional iodine alcohol. With the animal lying in the prone position on the operating table, two random-pattern flaps

CONTACT Zhi-Yong Bai ✉ zhybai_md@126.com 🖳 Department of Ultrasound, Beijing Tsinghua Changgung Hospital, #168, Litang Road, Changping District, Beijing 102218, P.R. China

#These authors contributed equally to this work.

deep to the fascia were raised on the back. Each flap was located 1.0 cm from the spinous process of the vertebrae. For the left side, the flap was 1.5 cm long and 1.5 cm wide and well-vascularized. For the right side, the flap was 9.0 cm long and 1.5 cm wide and was designed to lack blood perfusion. The 1.5-cm-wide pedicle of the right flap was located along the line joining the two iliac spines, and the ends of both sides of the flaps were on the same horizontal line (Figure 1). The flaps were then sutured back to the original position with 5-0 silk stitches. Each rat was housed in a single cage postoperatively.

Contrast-enhanced ultrasound

All the experimental rats were provided CEUS examinations within 12 h post operation for the blood supply evaluation in the early period postoperatively and received CEUS 7 days post operation when the circulation status stabilized. The CEUS examinations were performed by the same experienced ultrasound practitioner (HBZ).

All rats were placed in the prone position at room temperature (24°C). A catheter was placed in the caudal vein for contrast agent application. SonoVue™ powder (25.0 mg, Bracco, Milan, Italy) was dissolved in 5.0 mL of normal saline, and the microbubble concentration was approximately 2.0×10^8/mL. The microbubbles were infused at 50 μL/100 g/min. The steady-state conditions were achieved 2.0 min after the start of the infusion.

Figure 1. The flap design of the rat model. Two flaps were located symmetrically on both sides of the midline of the back. The short flap was designed as a viable flap, which had a width of 1.5 cm and a length of 1.5 cm. The long one was designed as a necrotic flap, which had a width of 1.5 cm and a length of 9.0 cm.

An ultrasound system (Aplio500, TOSHIBA, Japan) with a linear array L4–11 transducer (frequency range 4–11 MHz) was used for CEUS. The parameter settings were held constant throughout the experiment, which were as follows: frequency of 11 MHz, detection depth of 2.5 cm, focus position at 1.2 cm, gain of 80, dynamic range of 40, and frame rate of 5 Hz. For the two-dimensional (2D) mode, the mechanical index (MI) was 0.05. For the lost of correlation (LOC) mode, the MI was 1.53.

The skin flap and adjacent normal dorsal skin were imaged simultaneously in the axial plane. The real-time 2D ultrasound was performed with the low MI (0.05) first, then the flap was identified and the imaging was digitally recorded. After that, the LOC mode was used. The first frame with the high-power LOC pulse was digitally recorded and used for the analysis of the tissue blood volume (BV). Imaging was performed at two different flap territories, including the base and the end of the flap.

CEUS data analysis

With the standard online configuration software of this ultrasonic system, the tissue background signals were digitally subtracted from the imaging, and only the signals from the microbubbles corresponding to the microvascular BV were left. This background-subtracted image was stored in JPG format. Acoustic intensity (AI) was measured for the region of interest (ROI) in both flaps and the adjacent healthy skin using Image J 1.8.0 (National Institutes of Health, Bethesda, MD, USA). The ROI was a rectangle approximately 0.25 cm in length and 0.1 cm in height, avoiding regions adjacent to the suture line. The data were then expressed as a ratio of AI in the flap to that in the adjacent normal skin.

Flap survival area

Photographs of the two flaps were taken from the operative day to postoperative day 7. The digital images of the skin flaps were analyzed using Image-Pro Plus 6.0 (Media Cybernetics, Inc., Bethesda, MD, USA) to calculate the necrotic areas. The flap survival was calculated using the following formula [11]: flap survival = flap survival area / flap total area × 100%.

Hematoxylin and eosin and immunohistochemical staining

All rats were euthanized 7 days postoperatively. The 0.5-cm-long base and end of flaps of both sides were collected for each rat. These four skin samples were subjected to routine staining with hematoxylin and eosin (HE). Immunohistochemical (IHC) staining of α-smooth muscle actin was also performed for the arterioles count [11].

Most of the reagents were purchased from Beijing Zhongshan Golden Bridge Biotechnology Company (Beijing, China). Formalin-fixed, paraffin-embedded tissue sections (4.0 μm thick) underwent deparaffinization, stepwise rehydration, and endogenous peroxide blockage. For α-smooth muscle actin staining, slides were processed with antigen retrieval achieved by boiling the slides in citrate buffer (pH 6.0) for 1.5 min. Nonspecific binding was blocked using 10% nonimmune goat serum (ZLI-9021) for 10.0 min. Sections were incubated for 120.0 min at room temperature with α-smooth muscle actin antibody (ZM-0003) at a 1:100 dilution. After rinsing, the sections were incubated with secondary antibodies labeled with HRP (K5007, EnVision™ Detection System, Dako, Denmark) for 30.0 min at 37.0°C followed by visualization with DAB chromogen, counterstained with hematoxylin, dehydrated, and mounted. After rinsing again, these sections were

Table 1. Acoustic intensity ratio of flaps within 12 h post operation and 7 days post operation.

Grouping	Acoustic intensity ratio
Early stage (within 12 h)	
Short base	0.936 ± 0.182
Long base	0.884 ± 0.109
Short end	0.921 ± 0.141
Long end	0.442 ± 0.083
Late stage (after 7 days)	
Short base	0.858 ± 0.154
Long base	0.803 ± 0.103
Short end	0.814 ± 0.160
Long end	0.216 ± 0.124

incubated with alkaline phosphatase streptavidin (ZB-2422) at a 1:500 dilution for 60.0 min at 37.0 °C followed by visualization with BCIP/NBT (ZLI-9041), counterstained with eosin, dehydrated, and mounted. Negative controls were processed using the same procedure except the absence of the primary antibodies. No detectable staining was observed in any of the negative control slides.

In IHC staining of α-smooth muscle actin, the boundaries of arterioles were stained brown. Ten visual fields (200×) were chosen randomly in each slide of bases and ends of both sides flaps for arteriole count. Then, we calculated the mean count.

Statistical analysis

The data were analyzed using IBM SPSS Statistics 25.0 (International Business Machines Corp., USA) and expressed as the mean ± standard deviation. The data were analyzed using a paired sample T test, and significance was denoted by p values < 0.05.

Results

Microvascular BV

The AI ratios of the two flaps within 12 h post operation and 7 days post operation are shown in Table 1. For the early-stage group analysis, there was a greater value for the end of the short flap than that of the end of the long flap ($p < 0.001$), and there was also a greater value of the base of the long flap than the end of the long flap ($p < 0.001$),

which indicated the poor microvascular perfusion of the end of the long flaps. There was no difference in the AI ratio between the base of the short and the long flaps ($p > 0.05$), and there was also no difference between the base and the end of the short flaps ($p > 0.05$), which indicated that the microvascular perfusion of the end of the short flaps was as good as that of the pedicle (Figure 2). For the late-stage group analysis, the same results were presented.

Flap survival area

All the rats presented a steady increase in the necrosis size of the long flaps as time progressed, while no necrosis occurred in the short flaps (Figure 3). At 4–7 days postoperatively, when the necrotic areas were fixed, the long flaps showed $55.4 \pm 3.5\%$ mean survival areas, while the short flaps survived.

HE staining

In the bases of the long flaps, the structure of the dermomuscular layer was distinct, and there was some subcutaneous inflammatory cell infiltration. In the ends of the long flaps, the dermomuscular layer was atrophied, and there was a significant accumulation of inflammatory cells.

In the bases and ends of the short flaps, the tissue structure was normal with sufficient subcutaneous vasculature, and the muscle fibers of the dermomuscular layer were arranged regularly. There was infiltration of a few inflammatory cells (Figure 4).

Arteriole count of α-smooth muscle actin IHC staining

The arteriole distributions in the epidermis and subcutaneous connective tissue are shown in Figure 5. The arteriole counts of the ends and bases of both sides flaps are shown in Table 2. There were more arterioles in the ends of the short flaps than in the ends of the long flaps ($p < 0.001$), and there were also more arterioles in the bases of the long flaps than in the ends of the long flaps ($p < 0.001$). Nevertheless, there was no difference in arteriole count between the bases of the short flaps and the long flaps ($p > 0.05$), and there was also no difference in arteriole counts between the bases and the ends of the short flaps ($p > 0.05$).
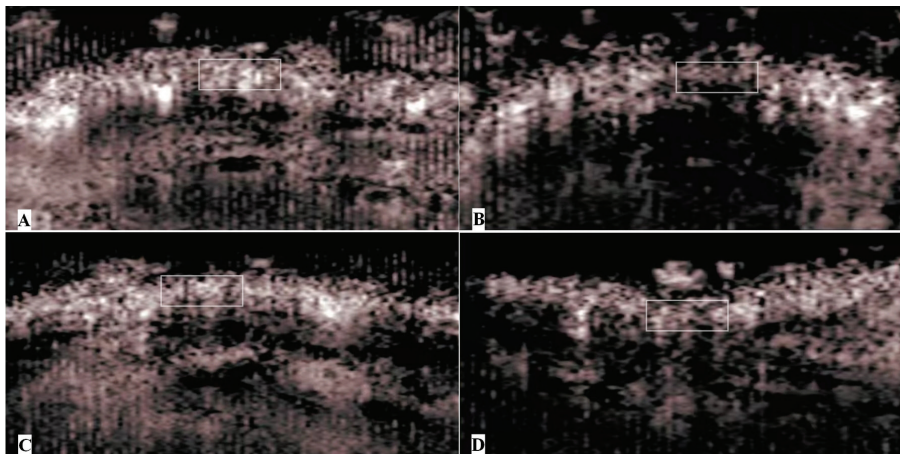
Figure 2. Images of CEUS within 12 h post operation. The portion of the flap was marked by the white rectangle. There were more bubble signals in the end of the short flap (A), the base of the short flap (C), and the base of the long flap (D). There were fewer bubble signals in the end of the long flap (B), which indicated poor microvascular perfusion. CEUS: contrast-enhanced ultrasound.

operative day   postoperative day 1   postoperative day 4   postoperative day 7
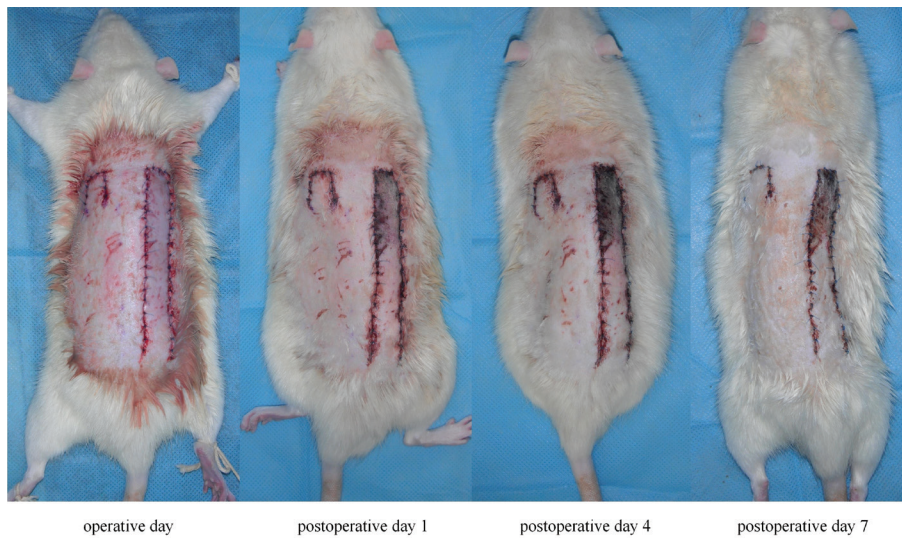
Figure 3. Consecutive observation of flaps post operation. The color of the long flap did not become dark until 24 h postoperatively, and the necrotic area of the long flap increased until 4 days postoperatively. Meanwhile, the short flap maintained its viability during the postoperative period.

Discussion

This study is a kind of confirmatory research. For this pair of well-designed random-pattern flaps model on the rat, the blood supply of the short flap should be good, and the distal end of the long flap should get poor blood perfusion as a result of exceeding the ordinary length to width ratio [12]. These predictable outcomes were confirmed by consecutive postoperative observation. The color of the distal part of the long flap started to become dark from 24 h postoperatively because of the shortage of blood supply, and the necrotic areas were fixed 4–7 days postoperatively. The results were also validated by HE staining and α-smooth muscle actin IHC staining of pathological sections.

The CEUS examination was performed within 12 h post operation for the blood supply evaluation in the early period postoperatively. The long flaps were checked for the poor circulation status of the end portions within 12 h postoperatively when compared to the base portions. It was much earlier to detect the sign of flap necrosis than the flap color observation, which demonstrated that the CEUS examination with the present parameters was sensitive enough to reveal the status of microcirculation of the random-pattern flaps. For the short flaps, which were well-designed as a viable pattern, early-stage CEUS also revealed no difference in the microvascular BV between the end and the base parts. This demonstrated the accuracy of the CEUS examination in microcirculation evaluation.

Moreover, when the necrotic areas of the long flaps were fixed at 7 days postoperatively while the short flaps survived, the arterioles count of α-smooth muscle actin IHC staining also indicated significantly fewer arterioles in the ends of the long flaps and a similar high level of arteriole count among the short bases, the short ends, and the long bases. Meanwhile, the CEUS examination, which was performed 7 days post operation, did reveal the corresponding perfusion status of both sides of the flaps precisely, which indicated that the CEUS examination in this study was reliable and that the results were accurate in the field of microcirculation monitoring.

For the parameter settings for CEUS, the most commonly used quantitative CEUS mode for tissue perfusion assessment was low-MI [13]. In low-MI CEUS imaging, the microbubbles are not destroyed
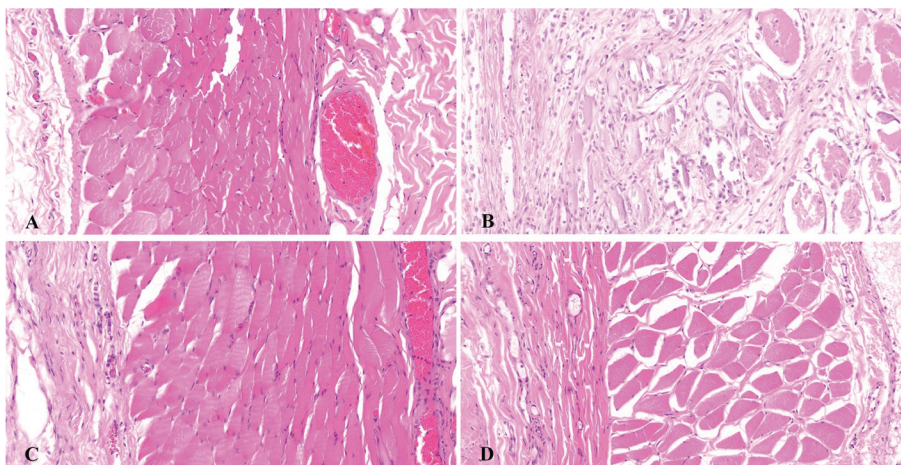
Figure 4. HE staining (200×) of both sides of the flaps 7 days post operation. The tissue structure was normal, with muscle fibers of the dermomuscular layer arranged regularly, and infiltration of a few inflammatory cells could be seen in the short flap end (A), short flap base (C), and long flap base (D). The dermomuscular layer was atrophied, the tissue structure could not be distinguished in the long flap end, and there was a significantly large amount of inflammatory cell infiltration (B).

Table 2. Arteriole count of flaps 7 days post operation.

Grouping	Arterioles (n)
Short base	6.73 ± 1.72
Long base	7.07 ± 2.49
Short end	6.50 ± 2.73
Long end	3.07 ± 2.23

but oscillate nonlinearly and give off continual backscattered intensity signals to be received by the ultrasound facility. Then, the time–intensity curve (TIC) of the ROI could be calculated. The tissue space resolution of ultrasound depends on transducer frequency, which means that a higher transducer frequency correlates with a higher tissue space resolution. The rat model flaps in this study were thin, with thicknesses of 2.0–4.0 mm. To obtain a better space resolution of flaps, a linear array transducer and high frequency of 11 MHz were used. However, the backscatter intensity of SonoVue™ varies with the ultrasound frequency in low-MI CEUS, which means that the backscatter intensity decreases with increasing frequency. It has been reported that the backscatter intensity of SonoVue™ bubbles decreases to 50% as the ultrasound frequency increases from 2 MHz to 5 MHz and even decreases to 25% with an ultrasound frequency of 10 MHz [14, 15].

As a result, it was found in the preliminary experiment that for this rat flap model and 11 MHz high transducer frequency, the flap space resolution was better enough, but the SonoVue™ bubble backscatter signals were too weak to be detected with low-MI CEUS. To obtain high-intensity backscatter signals with this 11 MHz high transducer frequency, a high-MI CEUS, also named flash imaging, was utilized in this perfusion evaluation for the random-pattern flap rat model.

Different from most low-MI TIC quantitative CEUS [10, 16–19], flashing imaging is a CEUS mode with high-MI that can destroy microbubbles and can greatly enhance the signal intensity amplitude [20]. In this ultrasound system (Aplio500, TOSHIBA, Japan), the flash imaging mode was also named the LOC mode. It was found in the preliminary experiment that with bubbles infused at 50 μL/100 g/min, high-intensity backscatter signals could be obtained and recorded. With the standard online configuration software of this ultrasonic system, the tissue background signal could be digitally subtracted from imaging, and only the transient flash signals from disrupted microbubbles were left, which could be used for microvascular BV evaluation.

Despite the promising results, there were still some limitations in this study. The monitoring of flap perfusion was not continuous during the postoperative period, so the reliability of this CEUS examination was slightly weak. Furthermore, the examination and findings depend highly upon the experience of the examiner.

Conclusions

Our findings indicated that the assessment of microcirculation with CEUS could provide valuable information on the viability of superficial tissues such as random-pattern flaps in a minimally invasive way. It could sensitively and accurately reveal the objective status of tissue perfusion even in the early stage after flap surgery, which would help guide subsequent treatment.

Ethical approval

The study was approved by the Animal Ethics Committee of the Peking University Health Science Center (ethics approval number: LA2013-83).
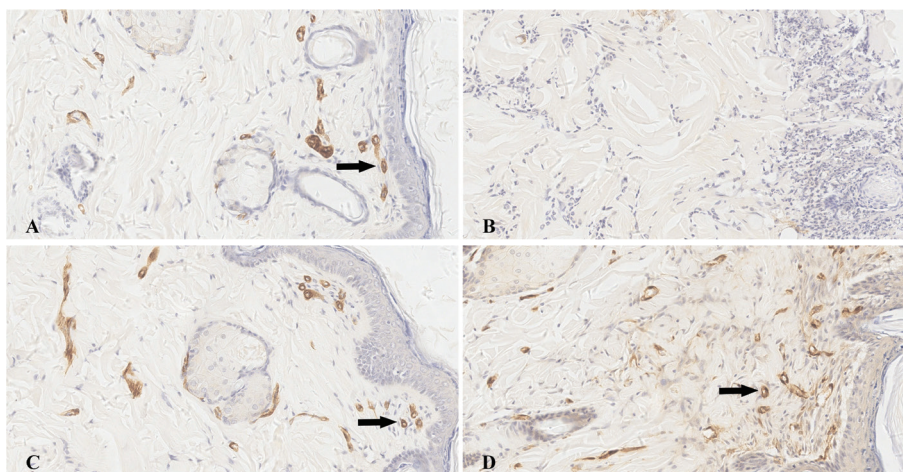
Disclosure statement

The authors report there are no competing interests to declare.

ORCID

Jian-Xun Ma https://orcid.org/0000-0003-3947-509X
You-Chen Xia https://orcid.org/0000-0001-5602-1319
Zhi-Yong Bai https://orcid.org/0000-0003-2947-5512
Hua-Bin Zhang https://orcid.org/0009-0003-4353-4627
Xia Xie https://orcid.org/0009-0001-3996-2456

Figure 5. α-smooth muscle actin immunohistochemical staining (200×) of both sides of the flaps 7 days post operation. The arteriole was characterized as a brown colored circle (black arrow). A certain amount of arterioles could be investigated in the epidermis and subcutaneous tissue of the short flap end (A), short flap base (C), and long flap base (D), and there was no obvious difference in the arteriole count number among them. There was almost no arteriole observed in the long flap end (B).

References

[1] Chen KT, Mardini S, Chuang DC, et al. Timing of presentation of the first signs of vascular compromise dictates the salvage outcome of free flap transfers. Plast Reconstr Surg. 2007;120:187–195. https://doi.org/10.1097/01.prs.0000264077.07779.50

[2] Disa JJ, Cordeiro PG, Hidalgo DA. Efficacy of conventional monitoring techniques in free tissue transfer: an 11-year experience in 750 consecutive cases. Plast Reconstr Surg. 1999;104:97–101. https://doi.org/10.1097/00006534-199907000-00014

[3] Kind GM, Buntic RF, Buncke GM, et al. The effect of an implantable Doppler probe on the salvage of microvascular tissue transplants. Plast Reconstr Surg. 1998;101:1268–1273. https://doi.org/10.1097/00006534-199804010-00016

[4] Smit JM, Acosta R, Zeebregts CJ, et al. Early reintervention of compromised free flaps improves success rate. Microsurgery. 2007;27:612–616. https://doi.org/10.1002/micr.20412

[5] Cai ZG, Zhang J, Zhang JG, et al. Evaluation of near infrared spectroscopy in monitoring postoperative regional tissue oxygen saturation for fibular flaps. J Plast Reconstr Aesthet Surg. 2008;61:289–296. https://doi.org/10.1016/j.bjps.2007.10.047

[6] Walle L, Sudhoff H, Frerichs O, et al. Intraluminal monitoring of micro vessels. A surgical feasibility study. Front Surg. 2021;8:681797. https://doi.org/10.3389/fsurg.2021.681797

[7] Wang D, Chen W. Indocyanine green angiography for continuously monitoring blood flow changes and predicting perfusion of deep inferior epigastric perforator flap in rats. J Invest Surg. 2021;34:393–400. https://doi.org/10.1080/08941939.2019.1641253

[8] Fellner C, Jung EM, Prantl L. Dynamic contrast-enhanced MRI as a valuable non-invasive tool to evaluate tissue perfusion of free flaps: preliminary results. Clin Hemorheol Microcirc. 2010;46:77–87. https://doi.org/10.3233/CH-2010-1335

[9] Dietrich CF, Averkiou M, Nielsen MB, et al. How to perform contrast-enhanced ultrasound (CEUS). Ultrasound Int Open. 2018;4:E2–E15. https://doi.org/10.1055/s-0043-123931

[10] Geis S, Prantl L, Schoeneich M, et al. Contrast enhanced ultrasound (CEUS) – an unique monitoring technique to assess microvascularization after buried flap transplantation. Clin Hemorheol Microcirc. 2016;62:205–214. https://doi.org/10.3233/CH-151964

[11] Ma JX, Yang QM, Xia YC, et al. Effect of 810 nm near-infrared laser on revascularization of ischemic flaps in rats. Photomed Laser Surg. 2018;36:290–297. https://doi.org/10.1089/pho.2017.4360

[12] Hansen SL, Young DM, Lang P, et al. Flap classification and applications. In: Gurtner GC, editor. Plastic surgery volumes one: principles. 3rd ed. London: Elsevier Saunders; 2013. p. 512.

[13] Prantl L, Geis S, Lamby P, et al. Recommendations for contrast enhanced ultrasound (CEUS) in free tissue transplant monitoring. Clin Hemorheol Microcirc. 2015;61:359–365. https://doi.org/10.3233/CH-152005

[14] Karshafian R, Bevan PD, Williams R, et al. Sonoporation by ultrasound-activated microbubble contrast agents: effect of acoustic exposure parameters on cell membrane permeability and cell viability. Ultrasound Med Biol. 2009;35:847–860. https://doi.org/10.1016/j.ultrasmedbio.2008.10.013

[15] Sun Y, Kruse DE, Dayton PA, et al. High-frequency dynamics of ultrasound contrast agents. IEEE Trans Ultrason Ferroelectr Freq Control. 2005;52:1981–1991. https://doi.org/10.1109/TUFFC.2005.1561667

[16] Mueller S, Wendl CM, Ettl T, et al. Contrast-enhanced ultrasonography as a new method for assessing autonomization of pedicle and microvascular free flaps in head and neck reconstructive surgery. Clin Hemorheol Microcirc. 2017;65:317–325. https://doi.org/10.3233/CH-16194

[17] Sangwan A, Goyal A, Kumar A, et al. Contrast enhanced ultrasound for characterization of suspected soft tissue vascular anomalies. Eur J Radiol. 2022;153:110370. https://doi.org/10.1016/j.ejrad.2022.110370

[18] Kehrer A, Mandlik V, Taeger C, et al. Postoperative control of functional muscle flaps for facial palsy reconstruction: ultrasound guided tissue monitoring using contrast enhanced ultrasound (CEUS) and ultrasound elastography. Clin Hemorheol Microcirc. 2017;67:435–444. https://doi.org/10.3233/CH-179224

[19] Geis S, Prantl L, Gehmert S, et al. TTP (time to PEAK) and RBV (regional blood volume) as valuable parameters to detect early flap failure. Clin Hemorheol Microcirc. 2011;48:81–94. https://doi.org/10.3233/CH-2011-1396

[20] Kamiyama N, Moriyasu F, Mine Y, et al. Analysis of flash echo from contrast agent for designing optimal ultrasound diagnostic systems. Ultrasound Med Biol. 1999;25:411–420. https://doi.org/10.1016/S0301-5629(98)00182-3